

Content-Aware RSMA-Enabled Pinching-Antenna Systems for Latency Optimization in 6G Networks

Yu Hua, Yaru Fu, Yalin Liu, Zheng Shi, Member, IEEE, Kevin Hung, Senior Member, IEEE

Abstract—The Pinching Antenna System (PAS) has emerged as a promising technology to dynamically reconfigure wireless propagation environments in 6G networks. By activating radiating elements at arbitrary positions along a dielectric waveguide, PAS can establish strong line-of-sight (LoS) links with users, significantly enhancing channel gain and deployment flexibility, particularly in high-frequency bands susceptible to severe path loss. To further improve multi-user performance, this paper introduces a novel content-aware transmission framework that integrates PAS with rate-splitting multiple access (RSMA). Unlike conventional RSMA, the proposed RSMA scheme enables users requesting the same content to share a unified private stream, thereby mitigating inter-user interference and reducing power fragmentation. We formulate a joint optimization problem aimed at minimizing the average system latency by dynamically adapting both antenna positioning and RSMA parameters according to channel conditions and user requests. A Content-Aware RSMA and Pinching-antenna Joint Optimization (CARP-JO) algorithm is developed, which decomposes the non-convex problem into tractable subproblems solved via bisection search, convex programming, and golden-section search. Simulation results demonstrate that the proposed CARP-JO scheme consistently outperforms Traditional RSMA, NOMA, and Fixed-antenna systems across diverse network scenarios in terms of latency, underscoring the effectiveness of co-designing physical-layer reconfigurability with intelligent communication strategies.

Index Terms—Pinching-antenna, latency minimization, power control, positioning, RSMA.

I. Introduction

The evolution towards sixth-generation (6G) wireless networks introduces stringent demands for massive connectivity, high capacity, and ultra-low latency, posing significant challenges to system spectral efficiency and

connection reliability. In high-frequency bands, such as millimeter-wave and terahertz, communication links are highly dependent on line-of-sight (LoS) conditions. However, obstacles in practical environments often lead to non-LoS scenarios and severe path loss. To address this, Pinching Antenna System (PAS) has emerged as a promising solution by dynamically reconfiguring wireless propagation environments. Specifically, PAS utilizes dielectric waveguides to guide electromagnetic waves, and pinching antenna (PA) can be activated at arbitrary points along the waveguide to establish strong LoS links with users, thereby significantly enhancing channel strength and flexibility of deployment [1]–[3]. Concurrently, at the multiple access layer, Rate-Splitting Multiple Access (RSMA) has emerged as a powerful and robust framework that generalizes and outperforms conventional schemes, such as Orthogonal Multiple Access (OMA) and Non-Orthogonal Multiple Access (NOMA) [4], [5]. By splitting user messages into common and private parts, RSMA efficiently manages multi-user interference, offering a superior trade-off between performance and receiver complexity.

Although the individual merits of PAS and RSMA are evident, existing research on their integration remains content-agnostic, which is a critical oversight. In modern networks, especially in video streaming and content distribution scenarios, the transmitted data is not merely anonymous bits but structured “content”, distinct files such as videos, songs, or software updates from a finite library. A key characteristic of content delivery is multicast; multiple users often request the same popular file simultaneously. However, conventional RSMA, even in such scenarios, generates a distinct private stream for each user, irrespective of whether they request the same content. This leads to the inefficient transmission of duplicate streams, creating unnecessary inter-user interference and fragmenting the limited transmit power across multiple streams for the same data. This power fragmentation and increased interference directly result in suboptimal data rates and, consequently, higher latency, which is the very metric 6G aims to minimize.

Therefore, the core motivation of this work is to bridge this gap by introducing content-awareness into the PAS-RSMA co-design. We propose that the system recognizes when users request the same content and adapts its transmission strategy accordingly. This paradigm shift, from user-aware to content-aware transmission, unlocks significant potential for latency reduction. Furthermore, the physical reconfigurability of PAS provides a unique

This work was supported in part by the Team-based Research Fund under Reference No. TBRF/2024/1.10, in part by the Research Matching Grant under Reference No. CP/2025/1.1, in part by the Hong Kong Metropolitan University Research & Development Project under Reference No. RD/2023/2.22, and in part by the grant from the Research Grants Council of the Hong Kong Special Administrative Region, China, under project No. UGC/FDS16/E15/24, and in part by Wuxi University Research Start-up Fund For High-level Talents 2025r030. (Corresponding author: Yaru Fu)

Y. Hua is with the School of Electronic Information and Engineering, Wuxi University, Wuxi, Jiangsu 214105, China and Jiangsu Province Engineering Research Center of Integrated Circuit Reliability Technology and Testing System, Wuxi, Jiangsu 214105, China (Email: 860474@cwuxu.edu.cn).

Y. Fu, Y. Liu, and K. Hung are with the School of Science and Technology, Hong Kong Metropolitan University, Hong Kong, 999077, China (E-mail: yfu@hkmu.edu.hk; ylliu@hkmu.edu.hk; khung@hkmu.edu.hk).

Z. Shi is with the School of Intelligent Systems Science and Engineering, Jinan University, Zhuhai 519070, China (e-mail: zhengshi@jnu.edu.cn).

spatial degree of freedom that can be jointly optimized with this content-aware RSMA strategy to further enhance the channel conditions for both common and private streams. The joint optimization of these cross-layer parameters, spanning the physical layer (antenna position) and the link layer (content-aware RSMA resource allocation), specifically for minimizing latency in a content-aware network, constitutes the central problem addressed in this paper.

A. Literature Review

Existing research on PAS has primarily focused on their fundamental capabilities and performance in single-user or basic multi-user scenarios. The seminal work in [1] introduced the core PAS concept, demonstrating that applying a plastic pinch to a dielectric waveguide enables efficient radio wave radiation in indoor environments. This was further expanded in [2], which provided a comprehensive overview of PAS principles, applications, and challenges, with particular emphasis on its potential to improve LoS communication and coverage extension. Authors in [3] developed a comprehensive 3D modeling and theoretical framework for PAS in indoor immersive communications, providing both performance analysis and practical deployment guidelines for 6G applications. Performance evaluations in [6] established PAS's superiority over conventional fixed-antenna systems in mitigating path loss, supported by detailed analyses of outage probability and average data rate. Building on this, authors in [7] investigated rate maximization in a downlink PAS through optimized antenna positioning to minimize path loss while ensuring constructive signal interference.

Recent studies have explored more advanced multi-user configurations and application scenarios. In [8], a matching algorithm was developed for joint waveguide assignment and antenna activation, strategically establishing LoS/NLoS links to enhance signals and suppress interference, thus significantly improving the sum rate. The authors in [9] revealed that LoS blockage can actually enhance PAS performance in multi-user scenarios by suppressing co-channel interference. For multi-waveguide configurations, the authors in [10] proposed a fractional programming approach to optimize antenna locations, achieving significant gains in uplink sum of rates while maintaining robustness to waveguide losses.

The application scope of PAS has expanded to encompass a diverse range of domains. In [11], a novel wireless sensing architecture integrating PAS with leaky coaxial cables was proposed, where a particle swarm optimization (PSO)-based algorithm jointly optimizes the transmit waveform and antenna positions to minimize the Cramér-Rao bound (CRB), demonstrating substantial improvements in sensing accuracy. Meanwhile, [12] applied maximum entropy reinforcement learning to joint antenna positioning and power optimization in PAS-enabled integrated sensing and communication (ISAC) systems, demonstrating superior performance in balancing communication rates and sensing requirements.

Collectively, these studies underscore the capability of PAS to enhance channel conditions through dynamic antenna placement. However, most existing works focus on single-user scenarios or simple orthogonal multiple access (OMA) schemes, leaving key challenges such as multi-user interference and resource allocation largely unaddressed. To address these challenges, advanced multiple access techniques, including non-orthogonal multiple access (NOMA) and rate-splitting multiple access (RSMA), have been integrated into PAS designs. NOMA, in particular, leverages power-domain multiplexing to serve multiple users within the same resource block, naturally aligning with the signal superposition characteristics inherent in waveguide-based PAS architectures. For instance, the work in [13] investigated sum-rate maximization in an uplink NOMA-assisted PAS, establishing its superior spectral efficiency compared to OMA schemes. Extending this line of research, [14] explored a NOMA-based PAS with discrete antenna activation, developing low-complexity algorithmic solutions for sum-rate optimization. Further advancing system efficiency, [15] introduced a convergent iterative algorithm for multi-waveguide NOMA-assisted PAS that minimizes total transmit power while revealing an oscillatory decay relationship between the optimal power and waveguide spacing. For wireless powered communications, the authors in [16] investigated PAS-assisted networks with both TDMA and NOMA protocols, developing high-performance element-wise (EW) and low-complexity stochastic parameter differential evolution (SPDE) algorithms that achieve optimal performance with a PA power distribution ratio of 0.55-0.6.

However, the practical implementation of NOMA imposes a significant computational burden, particularly on users with strong channel conditions. These users are required to sequentially decode and cancel the signals intended for all weaker users via successive interference cancellation (SIC) before accessing their own information. This process introduces considerable processing complexity and latency, which becomes prohibitive as the number of users increases [17]. To mitigate these inherent limitations of NOMA, RSMA has been advanced as a more flexible and robust alternative [18]–[20]. In a downlink RSMA system, each user's message is split into a common part and a private part. The base station consolidates all common parts into a single common stream, while encoding each private part into an individual stream. All streams are then superimposed for transmission. At the receiver, each user first decodes the common stream, subtracts it via SIC, and then proceeds to decode its designated private stream while treating other private streams as noise. A key advantage of RSMA lies in its ability to manage complexity by adjusting the message-splitting ratios, offering a superior balance between interference management and decoding overhead.

Studies have corroborated its benefits, for example, in [21], an RSMA-based UAV communication system was proposed where joint optimization of scheduling, rate allocation, power control, and UAV trajectory was solved

via a block coordinate descent approach, demonstrating superior energy efficiency and user fairness compared to OMA and NOMA schemes. In [22], a low complexity user-pairing strategy was proposed for uplink RSMA to minimize maximum latency, achieving performance comparable to optimal RSMA while significantly reducing computational complexity compared to exhaustive search of the decoding order. In [23], an online optimization framework using Lyapunov optimization and successive convex approximation was developed for RSMA-based UAV networks, effectively minimizing energy consumption while guaranteeing throughput requirements for mobile ground users through joint trajectory design and resource allocation. As shown in [24], RSMA-based PAS with multiple waveguides achieved higher sum rates compared to NOMA and conventional SDMA, thanks to its ability to reduce spatial correlation and enhance common stream rates. Furthermore, authors in [25] derived closed-form outage probability expressions for uplink RSMA-PAS, validating its superiority over NOMA in terms of reliability and flexibility.

Despite these advancements, a significant limitation persists: existing multiple-access PAS frameworks are not content-aware. They cannot handle redundancy in user requests, leading to inefficient transmission of duplicate private streams and unnecessary interference. Consequently, this results in suboptimal latency performance, especially in multicast scenarios with popular content. Furthermore, the joint optimization of the pinching antenna's physical location and content-aware RSMA's resource allocation specifically for latency minimization remains an open challenge.

B. Our Contributions

To bridge these gaps, this paper proposes a novel content-aware RSMA-enabled pinching-antenna scheme that jointly optimizes antenna positioning and advanced content-aware RSMA's resource allocation to minimize average latency in multicast downlink systems. Unlike existing studies, our approach introduces a content-aware stream-sharing mechanism in RSMA where users requesting the same file share the same private stream, thereby reducing inter-user interference and power fragmentation. The main contributions of this work are summarized as follows:

- We propose a novel content-aware RSMA-enabled downlink pinching-antenna framework, which integrates the spatial flexibility of the pinching antenna with a content-aware transmission strategy. In the advanced content-aware RSMA strategy, users who request the same content share a unified private stream. This design dramatically reduces inter-user interference and improves power efficiency, achieving superior performance particularly when user requests are concentrated. Furthermore, the private rate can be further improved by optimizing the position of the pinching antenna. For the common stream, all

users need to decode it, so the common rate is limited by the user with the worst channel condition. By adjusting the position of the pinching antenna, the channel quality of the worst-case user can be improved, thereby enhancing the common rate.

- With the novel framework, we formulate the average latency minimization problem via a joint pinching antenna's location and advanced RSMA resource allocation perspective. The formulated problem is a nonconvex problem, and all variables are mutually coupled, which is difficult to solve directly.
- To make it tractable, we develop a Content-Aware RSMA and Pinching-antenna Joint Optimization (CARP-JO) algorithm, which decomposes the original problem into two subproblems: the advanced RSMA resource allocation subproblem and the antenna positioning subproblem.
- For the advanced RSMA resource allocation subproblem, we optimize power and rate by employing alternating optimization between private power control via bisection and common rate allocation via convex programming, coupled with a one-dimensional search over the common stream power. For the antenna positioning subproblem, we determine the optimal location through a golden-section search along the waveguide, solving a convex rate allocation problem at each candidate position to evaluate the system latency.

Extensive simulation results validate that our scheme significantly outperforms Traditional RSMA, NOMA, and Fixed antenna systems in various network scenarios, including changes in transmit power, user density, and coverage size.

The remainder of this article is structured as follows: Section II introduces the system model of the advanced RSMA-driven pinching antenna network under consideration, along with the principles of content transmission. Section III provides a detailed formulation of the problem, while Section IV presents the proposed efficient joint optimization framework. Extensive performance evaluations and comparisons are discussed in Section V. Finally, Section VI concludes the paper and outlines potential directions for future research. For brevity, the notations used throughout this paper are summarized in Table I.

II. System Model

We investigate a downlink PAS where a base station (BS) serves a set of K users, as illustrated in Fig. 1. The BS employs a single dielectric waveguide of length L_W for transmission, with a pinching antenna activated at a specific point along it to establish LoS connections with the users, denoted by the set $\mathcal{K} = \{1, \dots, K\}$. The system operates in a 3D Cartesian coordinate system: the waveguide is aligned along the x -axis at a fixed height d , while the users are randomly distributed within a rectangular service area of dimensions $D_x \times D_y$ in the x - y plane. The location of the pinching antenna is $\Phi^{\text{Pin}} = (x^{\text{Pin}}, 0, d)$,

TABLE I: Notations and Descriptions

Notation	Description
K	The number of users
I	The number of contents
\mathbf{f}_k	The content request distribution for user
m_k	The requested content state of user k
L_W	The length of dielectric waveguide
$D_x \times D_y$	The side length of the user distribution area
Φ^{Pin}	The location of the pinching antenna
Φ_k	The location of user k
h_k	The channel between the antenna and user k
c	The speed of light
f_c	The carrier frequency
$\mathcal{I}(\mathbf{m})$	The collection of distinct files under request state \mathbf{m}
\mathcal{K}_i	The user cohort requesting file i
P_i	The power for private part of content i
P_0	The common stream power
h_0	The worst-case channel gain
R_0	The common stream rate
r_i	The common rate allocation to content i
$R_{i,r}$	The rate of the private stream s_i
R_i	The total achievable rate for content i
c_i	The data size of content i
L_{RSMA}	Overall transmission latency for all users
\mathbf{P}	The RSMA power control policy
\mathbf{r}	The common rate allocation vector

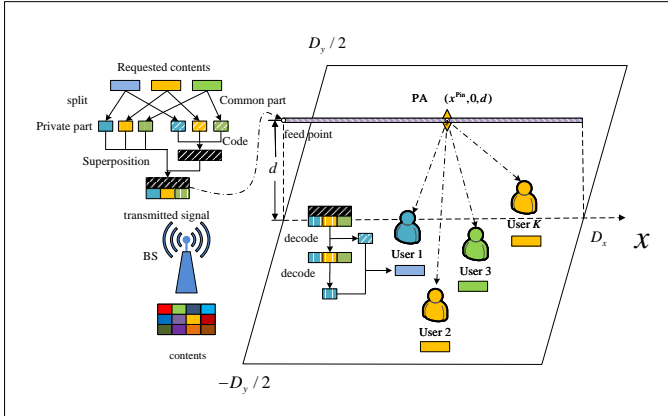


Fig. 1: System model of the considered content-aware RSMA-enabled PAS.

and the location of user k is $\Phi_k = (x_k, y_k, 0)$, where $x_k \in [0, D_x]$ and $y_k \in [-D_y/2, D_y/2]$ for all $k \in \mathcal{K}$.

A. Content Request Model

The BS maintains a content library $\mathcal{I} = \{1, 2, \dots, I\}$, consisting of I distinct files. Each content $i \in \mathcal{I}$ is characterized by a data size $c_i > 0$. The content request distribution for user k is represented by the vector $\mathbf{f}_k = (f_k(1), f_k(2), \dots, f_k(I))$, which follows a Zipf distribution [26] and $\sum_{i=1}^I f_k(i) = 1$. Let $m_k \in \mathcal{I}$ denote the content requested by user k , with the request probability given

by $f_k(m_k)$, $m_k \in \mathcal{I}$. User requests are assumed to be independent, thus the joint request state of the system is defined as $\mathbf{m} = (m_k)_{k \in \mathcal{K}} \in \mathcal{I}^K$. Let $f(\mathbf{m})$ be the probability mass function of the joint request state \mathbf{m} , which is given by

$$f(\mathbf{m}) = \prod_{k \in \mathcal{K}} f_k(m_k). \quad (1)$$

B. Channel Model

The channel between the BS and users in the PAS is characterized by a unique two-hop transmission process: the signal first propagates along the dielectric waveguide from BS to PA and is then radiated to the users via PA. Let $\Phi^{\text{BS}} = (0, 0, d)$ be the location of the feed point on BS. The signal fed into the waveguide at the feed point Φ^{BS} propagates along the waveguide to PA Φ^{Pin} . This process incurs a phase shift, which is modeled by the complex gain between the feed point Φ^{BS} and PA Φ^{Pin} [3]:

$$h_{\uparrow} = e^{-j \frac{2\pi}{\lambda_g} \|\Phi^{\text{BS}} - \Phi^{\text{Pin}}\|}, \quad (2)$$

where $\lambda_g = \lambda/n_{\text{eff}}$ is the guided wavelength, n_{eff} is the effective refractive index of the dielectric waveguide, and $\|\Phi^{\text{BS}} - \Phi^{\text{Pin}}\|$ is the propagation distance within the waveguide. The PA then radiates the signal into the free space, the channel between the PA at Φ^{Pin} and user k at Φ_k is accurately characterized by the free-space path loss model [3]:

$$h_{\downarrow,k} = \frac{\sqrt{\eta} e^{-j \frac{2\pi}{\lambda} \|\Phi^{\text{Pin}} - \Phi_k\|}}{\|\Phi^{\text{Pin}} - \Phi_k\|}, \quad (3)$$

where $\eta = \lambda^2/(16\pi^2)$ is the channel power gain at a reference distance of 1 m.

The overall channel gain for user k is the product of the waveguide propagation gain and the free-space radiation gain. Considering that the phase terms are compensated or averaged out in power calculations for system-level optimization [3], the effective channel gain of user k used for resource allocation, referred to as h_k , is expressed as follows:

$$h_k = |h_{\uparrow} \cdot h_{\downarrow,k}|^2 = \frac{\eta}{\|\Phi^{\text{Pin}} - \Phi_k\|^2}. \quad (4)$$

This simplified yet accurate model is justified by the PAS's operational principle, the dynamic positioning of the PA ensures a strong and stable LoS path, making the received power predominantly determined by the distance-dependent path loss. This model provides a tractable foundation for the subsequent joint optimization of antenna positioning and RSMA parameters.

C. Advanced RSMA Transmission Model

In traditional RSMA implementations, each user's message undergoes a segmentation process, splitting into common and private components. The common segments from all users undergo superposition coding to form a unified common stream s_0 , decoded via a codebook shared across all receivers. Meanwhile, each private segment is independently encoded into a dedicated private stream per

user. Crucially, even when multiple users request identical content, each receiver still obtains a distinct private stream. This approach inherently generates substantial inter-user interference. Furthermore, given the base station's finite transmit power, replicating private streams for identical content requests fragments the available power resources. Consequently, the transmission power allocated to individual users becomes critically low.

Mitigating private stream interference is achieved by having users requesting identical content share a common private part. For a given request state \mathbf{m} , define $\mathcal{I}(\mathbf{m})$ as the collection of distinct files requested. Each content $i \in \mathcal{I}(\mathbf{m})$ has its private segment multicast via a dedicated private stream s_i . Let \mathcal{K}_i denote the user cohort that requests file i , implying that these users share the stream s_i . The transmit power allocated to content i is denoted P_i , and P_0 is the transmit power allocated to common stream s_0 . Crucially, the number of distinct requested files cannot exceed the user count: $|\mathcal{I}(\mathbf{m})| \leq K$ where $|\mathcal{I}(\mathbf{m})|$ counts unique requested files. The transmitted signal is:

$$s = \sqrt{P_0}s_0 + \sum_{i \in \mathcal{I}(\mathbf{m})} \sqrt{P_i}s_i. \quad (5)$$

This structure substantially reduces private stream transmissions in advanced RSMA. Under BS power constraints, concentrating power allocation yields higher per-stream transmission power, consequently enhancing achievable rates.

1) Common Stream Rate: Universal decoding of the common stream s_0 mandates adherence to the limiting user channel. The worst-case channel gain $h_0 = \min_{k \in \mathcal{K}} h_k$ governs the common stream rate R_0 , which must satisfy:

$$R_0 = B \log_2 \left(1 + \frac{P_0}{\sum_{i \in \mathcal{I}(\mathbf{m})} P_i + \frac{\sigma^2}{h_0}} \right), \quad (6)$$

where B is the bandwidth, P_0 designates the common stream power and P_i signifies the private stream power for content i (per prior definition). In addition, σ^2 expresses the power of additive white Gaussian noise (AWGN). The common rate R_0 is allocated to the different contents. Let r_i denote the common rate allocated to content $i \in \mathcal{I}(\mathbf{m})$. These allocated rates r_i are non-negative and must satisfy the following sum constraint:

$$\sum_{i \in \mathcal{I}(\mathbf{m})} r_i \leq R_0, \quad r_i \geq 0. \quad (7)$$

2) Private Stream Rate: After successfully decoding the common stream s_0 , each user proceeds to decode the private stream associated with its requested content. The rate of the private stream s_i is denoted by $R_{i,r}$. To guarantee successful decoding of s_i by all users in \mathcal{K}_i , the rate $R_{i,r}$ must satisfy the following expression:

$$R_{i,r} = B \log_2 \left(1 + \frac{P_i}{\sum_{j \in \mathcal{I}(\mathbf{m}), j \neq i} P_j + \frac{\sigma^2}{\min_{k \in \mathcal{K}_i} h_k}} \right). \quad (8)$$

While serving users with poor channel conditions may appear to diminish achievable rates, the advanced RSMA

scheme enhances private stream rates by reducing the number of distinct private streams, thereby concentrating available transmit power on each remaining stream.

3) SIC Feasibility Condition: To ensure successful successive interference cancellation (SIC) [27], the following condition must be satisfied:

$$P_0 \geq \frac{P_b}{2} + \frac{\sigma^2 + \theta}{h_0}, \quad (9)$$

where θ denotes the minimum required power difference between the common stream power and the combined power of residual signals and noise. Additionally, P_b corresponds to the total power budget available at the BS.

D. Latency Model

Based on the above analysis, the total achievable rate R_i for content i comprises both the common and private stream rates, and is obtained as:

$$R_i = r_i + R_{i,r}, \quad i \in \mathcal{I}(\mathbf{m}). \quad (10)$$

This work aims to minimize the average latency of the system. Denote by L_{RSMA} the overall transmission latency for all users. The system latency under each request state is determined by the maximum latency among all requested contents, which is defined as:

$$L_{\text{RSMA}} = \max_{i \in \mathcal{I}(\mathbf{m})} \frac{c_i}{R_i}. \quad (11)$$

III. Problem Formulation and Analysis

This section details the mathematical formulation of the latency minimization problem and analyzes its inherent challenges. First, we formally present the joint optimization problem that integrates pinching-antenna positioning with content-aware RSMA resource allocation. Subsequently, we analyze the key difficulties in solving this problem, including its non-convexity and the strong coupling among variables, which motivates the design of our proposed alternating optimization framework.

A. Problem Formulation

This paper aims to minimize the average latency in content-aware RSMA-enabled pinching-antenna networks by jointly optimizing antenna positioning and advanced RSMA resource allocation strategies. For notational simplicity, let $\mathbf{P} = (P_i)_{i \in \mathcal{I}(\mathbf{m}) \cup 0}$ represent the RSMA power control policy, and $\mathbf{r} = (r_i)_{i \in \mathcal{I}(\mathbf{m})}$ denote the common rate allocation vector. Notably, the content-oriented RSMA resource allocation and the pinching-antenna location are adaptive to the request state \mathbf{m} . Therefore, we express these dependencies as $\mathbf{P}(\mathbf{m})$, $\mathbf{r}(\mathbf{m})$, and $x^{\text{Pin}}(\mathbf{m})$. The average system latency, denoted by $L(x^{\text{Pin}}, \mathbf{P}, \mathbf{r})$, is consequently calculated as:

$$\begin{aligned} L(x^{\text{Pin}}, \mathbf{P}, \mathbf{r}) &= \mathbb{E}[L_{\text{RSMA}}(x^{\text{Pin}}(\mathbf{m}), \mathbf{P}(\mathbf{m}), \mathbf{r}(\mathbf{m}))], \\ &= \sum_{\mathbf{m} \in \mathcal{M}} f(\mathbf{m}) \cdot \max_{i \in \mathcal{I}(\mathbf{m})} \frac{c_i}{R_i}, \end{aligned} \quad (12)$$

where \mathbf{M} denotes the set of all possible cases of \mathbf{m} , \mathbb{E} represents the expectation operator over all possible request states within $\mathbf{M} \in \mathcal{I}^K$.

Based on the above definitions, the average latency minimization problem is formally established as follows¹:

$$P0: \min_{x^{\text{Pin}}, \mathbf{P}, \mathbf{r}} L(x^{\text{Pin}}, \mathbf{P}, \mathbf{r})$$

$$\text{s.t.} \quad \sum_{i \in \mathcal{I}(\mathbf{m})} P_i + P_0 \leq P_b, \quad \mathbf{m} \in \mathbf{M}, \quad (13a)$$

$$\sum_{i \in \mathcal{I}(\mathbf{m})} r_i \leq R_0, \quad \mathbf{m} \in \mathbf{M}, \quad (13b)$$

$$P_0 \geq \frac{P_b}{2} + \frac{\sigma^2 + \theta}{h_0}, \quad (13c)$$

$$x^{\text{Pin}} \in [0, L], \quad (13d)$$

$$P_i \geq 0, \quad i \in \mathcal{I}(\mathbf{m}) \cup \{0\}, \quad \mathbf{m} \in \mathbf{M}, \quad (13e)$$

$$r_i \geq 0, \quad i \in \mathcal{I}(\mathbf{m}), \quad \mathbf{m} \in \mathbf{M}, \quad (13f)$$

where constraint (13a) imposes the total power budget limitation at the BS. (13b) restricts the aggregate common rate allocation. (13c) ensures the feasibility of SIC. (13d) confines the antenna position to the length of the dielectric waveguide. Constraints (13e) and (13f) impose non-negativity requirements on the corresponding decision variables.

B. Problem Analysis

1) Challenges: The formulated average latency minimization P0 is challenging to solve directly due to its inherent non-convexity and the strong coupling among the optimization variables. Specifically, the following challenges are identified: i) Non-convexity and NP-hardness. The objective function involves a max-of-ratio structure over multiple users and content items, while the constraints include non-convex expressions in both the rate and power variables. This makes P0 a non-convex optimization problem, which is generally NP-hard. ii) Strong coupling among variables. The pinching antenna position x^{Pin} affects all user channel gains, thereby coupling the physical layer configuration with the higher-layer resource allocation. Meanwhile, the RSMA power and rate variables are mutually interdependent, making it difficult to optimize them separately. iii) Extensive and mixed decision space. The problem involves both continuous variables (e.g., power, rate, antenna position) and discrete-like dependencies (e.g., content-aware stream grouping), leading to a complex mixed-integer non-linear programming (MINLP) structure.

2) Motivation for the Proposed Approach: The aforementioned challenges stimulate the design of a low-complexity and high-efficiency algorithm. Our proposed solution, an Alternating Optimization (AO) framework, is guided by the following key motivations:

- i) Tackling NP-hardness and Non-convexity. The NP-hard and non-convex nature of P0 makes finding a

global optimum computationally prohibitive. While machine learning algorithms like deep reinforcement learning (DRL) are alternatives, the mixed and coupled decision spaces in P0 would lead to complex action spaces, requiring extensive environmental interactions and suffering from long convergence times. In contrast, our proposed AO framework decomposes the problem into tractable subproblems, enabling efficient and stable convergence to a high-quality suboptimal solution.

- ii) Decoupling Interdependent Variables. The tight coupling among optimization variables necessitates a co-design approach. However, solving them simultaneously is intractable. This motivates us to decouple P0 into manageable subproblems: the RSMA resource allocation subproblem for a fixed antenna position and the antenna positioning subproblem under given RSMA parameters. This decomposition effectively breaks the coupling, allowing us to leverage powerful convex optimization and one-dimensional search techniques for each subproblem.
- iii) Balancing Complexity and Performance. When decomposing the problem, the extensive decision space poses a challenge in trading off complexity reduction and performance degradation. Dividing the problem into more subproblems lowers computational complexity but may narrow the solution space. Our decomposition strategy is driven by the need to reduce problem complexity while maintaining satisfactory performance. Specifically, we retain the joint optimization of power and rate within the RSMA subproblem due to their strong interaction, while separately optimizing the antenna position, which operates on a different spatial domain. This structure captures the most critical couplings while ensuring computational efficiency.

IV. Algorithms Design

This section presents the Content-Aware RSMA and Pinching-antenna Joint Optimization (CARP-JO) algorithm to solve the formulated P0. Owing to the non-convex nature of L_{RSMA} with respect to both x^{Pin} and \mathbf{P} , P0 is non-convex. As previously noted, all optimization variables are contingent upon the request state \mathbf{m} . Consequently, each distinct state necessitates independent variable optimization. To address this, we first consider a representative state $\mathbf{m} \in \mathbf{M}$, transform P0 into P0', and solve it to obtain the minimal latency for that state. The overall average system latency is subsequently evaluated by aggregating results across all states according to equation (12). Therefore, in the following context, unless otherwise specified, we will focus on a specific state \mathbf{m} . To make the subsequent optimization problems more concise, the constraint condition $\mathbf{m} \in \mathbf{M}$ for \mathbf{m} will be omitted. The P0' is given as follows:

$$P0': \min_{x^{\text{Pin}}, \mathbf{P}, \mathbf{r}} L_{\text{RSMA}}$$

¹Note that all variables inherently depend on \mathbf{m} ; the simplified notation is adopted for clarity.

$$\begin{aligned}
\text{C1} : & \sum_{i \in \mathcal{I}(\mathbf{m})} P_i + P_0 \leq P_b, \\
\text{C2} : & \sum_{i \in \mathcal{I}(\mathbf{m})} r_i \leq R_0, \\
\text{C3} : & P_0 \geq \frac{P_b}{2} + \frac{\sigma^2 + \theta}{h_0}, \\
\text{C4} : & x^{\text{Pin}} \in [0, L], \\
\text{C5} : & P_i \geq 0, i \in \mathcal{I}(\mathbf{m}) \cup \{0\}, \\
\text{C6} : & r_i \geq 0, i \in \mathcal{I}(\mathbf{m}).
\end{aligned}$$

It can be seen from constraint C2 that the three variables are mutually coupled, making it difficult to solve directly. Therefore, we split the P0' into two subproblems: the resource allocation subproblem for RSMA and the pinching-antenna location optimization subproblem.

A. Resource Allocation of Advanced RSMA

This subsection addresses the resource allocation subproblem for RSMA under a fixed antenna location x^{Pin} , denoted as P1. The formulation is as follows:

$$\begin{aligned}
\text{P1} : & \min_{\mathbf{P}, \mathbf{r}} \max_{i \in \mathcal{I}(\mathbf{m})} \frac{c_i}{R_i} \\
\text{s.t.} & \text{ C1, C2, C3, C5, C6.}
\end{aligned}$$

To enhance tractability, an auxiliary variable μ is introduced such that $\mu \geq \frac{c_i}{R_i}$ for all $i \in \mathcal{I}(\mathbf{m})$. Then, P1 can be reformulated as:

$$\begin{aligned}
\text{P1}' : & \min_{\mathbf{P}, \mathbf{r}, \mu} \mu \\
\text{s.t.} & \text{ C1, C2, C3, C5, C6,} \\
& \text{C7} : \frac{c_i}{R_i} \leq \mu, i \in \mathcal{I}(\mathbf{m}).
\end{aligned}$$

To efficiently solve P1', we first initialize a feasible value for P_0 . With P_0 fixed, we then perform alternating optimization between the common rate vector \mathbf{r} and the private power allocation vector $\mathbf{P}_r \triangleq (P_i)_{i \in \mathcal{I}(\mathbf{m})}$. Finally, a one-dimensional search over P_0 is conducted to determine its optimal value along with the corresponding optimal \mathbf{r} and \mathbf{P}_r .

1) Private Power Control Algorithm: Given a fixed common rate allocation vector \mathbf{r} , the private power allocation subproblem is formulated as:

$$\begin{aligned}
\text{P1.1} : & \min_{\mathbf{P}_r, \mu} \mu \\
\text{s.t.} & \text{ C1, C5, C7.}
\end{aligned}$$

Define $N_i = \frac{\sigma^2}{\min_{k \in \mathcal{K}_i} h_k}$ and $P_{\text{pri}} = P_b - P_0$. For $i \in \mathcal{I}(\mathbf{m})$, constraint C7 can be rewritten as:

$$R_i \geq \frac{c_i}{\mu}, \quad (14)$$

$$B \log_2 \left(1 + \frac{P_i}{\sum_{j \in \mathcal{I}(\mathbf{m}), j \neq i} P_j + N_i} \right) \geq \frac{c_i}{\mu} - r_i, \quad (15)$$

$$B \log_2 \left(\frac{P_{\text{pri}} + N_i}{P_{\text{pri}} + N_i - P_i} \right) \geq \frac{c_i}{\mu} - r_i. \quad (16)$$

Let $\Psi_i = P_{\text{pri}} + N_i$, then constraint C7 becomes:

$$\text{C7}' : B \log_2(\Psi_i - P_i) + \frac{c_i}{\mu} \leq B \log_2(\Psi_i) + r_i, \quad i \in \mathcal{I}(\mathbf{m}). \quad (17)$$

Thus, P1.1 is reformulated as:

$$\begin{aligned}
\text{P1.1}' : & \min_{\mathbf{P}_r, \mu} \mu \\
\text{s.t.} & \text{ C1, C5, C7}'.
\end{aligned}$$

P1.1' is non-convex due to the structure of constraint C7'. Although the objective is linear in μ and hence convex, the constraint involves the sum of a concave term $B \log_2(\Psi_i - P_i)$ and a convex term c_i/μ , which together do not yield a convex feasible region. Nevertheless, the problem can be efficiently solved via the bisection method by exploiting the monotonicity of μ . For a fixed μ , constraint C7' simplifies to:

$$\text{C7.1} : P_i \geq \Psi_i \left(1 - 2^{\frac{r_i}{B} - \frac{c_i}{\mu B}} \right), \quad i \in \mathcal{I}(\mathbf{m}). \quad (18)$$

The resulting problem for fixed μ becomes:

$$\begin{aligned}
\text{P1.1}^\dagger : & \min_{\mathbf{P}_r, \mu} \mu \\
\text{s.t.} & \text{ C1, C5, C7.1.}
\end{aligned}$$

To apply bisection, the upper and lower bounds of μ must be established. A natural lower bound is $\mu_{\text{low}} = 0$. The upper bound μ_{high} is derived from constraint C7 under the worst-case scenario where $P_i = 0$, i.e., $\mu_{\text{high}} = \max_{i \in \mathcal{I}(\mathbf{m})} \frac{c_i}{r_i}$. The bisection procedure is then carried out as follows: at each iteration, compute the midpoint $\mu_{\text{mid}} = (\mu_{\text{low}} + \mu_{\text{high}})/2$, and check the feasibility of P1.1[†]. If feasible, set $\mu_{\text{high}} = \mu_{\text{mid}}$; otherwise, set $\mu_{\text{low}} = \mu_{\text{mid}}$. The process continues until convergence. For clarity, the detailed procedure is summarized in Algorithm 1.

Algorithm 1 Joint Optimization Algorithm for P1.1

Require: Initial rate allocation \mathbf{r} and the common stream power P_0

- 1: Set $\mu_{\text{low}} = 0$, $\mu_{\text{high}} = \max_{i \in \mathcal{I}(\mathbf{m})} \frac{c_i}{r_i}$.
 - 2: repeat
 - 3: Let $\mu_{\text{mid}} = (\mu_{\text{low}} + \mu_{\text{high}})/2$, check the feasibility of P1.1[†] by CVX
 - 4: If feasible, set $\mu_{\text{high}} = \mu_{\text{mid}}$, and record a feasible solution \mathbf{P}_r
 - 5: otherwise, set $\mu_{\text{low}} = \mu_{\text{mid}}$
 - 6: until $|\mu_{\text{low}} - \mu_{\text{high}}| \leq \epsilon_1$
 - 7: return Optimized variables \mathbf{P}_r
-

2) Rate Allocation Algorithm: With the private power allocation vector \mathbf{P}_r held fixed, the original constraint C7' can be rearranged into a more tractable form as follows:

$$\text{C7.2} : r_i - \frac{c_i}{\mu} \geq -R_{i,r}. \quad (19)$$

This rearrangement leads to the formulation of the rate allocation subproblem, denoted as **P1.2**:

$$\text{P1.2} : \min_{\mathbf{r}, \mu} \mu$$

$$\begin{aligned} \text{s.t. C2: } & \sum_{i \in \mathcal{I}(\mathbf{m})} r_i \leq R_0, \\ \text{C6: } & r_i \geq 0, \quad i \in \mathcal{I}(\mathbf{m}), \\ \text{C7.2: } & r_i - \frac{c_i}{\mu} \geq -R_{i,r}, \quad i \in \mathcal{I}(\mathbf{m}). \end{aligned}$$

A detailed convexity analysis of problem **P1.2** reveals its well-structured nature. The objective function is linear in μ , and therefore convex. The constraint C2 is a linear inequality, while C6 consists of linear non-negativity constraints, both of which are convex. The key insight lies in analyzing the structure of constraint C7.2. The term $\frac{c_i}{\mu}$ is convex in μ for $\mu > 0$ since c_i is a positive constant, making its second derivative with respect to μ positive. Consequently, $-\frac{c_i}{\mu}$ is concave. As r_i is linear, the entire left-hand side expression $r_i - \frac{c_i}{\mu}$ is concave. A constraint where a concave function is greater than or equal to a constant (here $-R_{i,r}$) defines a convex feasible set.

Therefore, problem **P1.2** minimizes a linear objective subject to convex constraints, confirming it is a convex optimization problem. This favorable structure guarantees that any locally optimal solution is also globally optimal and allows the problem to be efficiently and reliably solved to global optimality using standard convex optimization tools such as CVX.

3) Joint Resource Allocation: Under a fixed common stream power allocation P_0 , the joint optimization of the common rate vector \mathbf{r} and the private power allocation vector \mathbf{P}_r is performed using an alternating optimization framework. This approach iteratively and alternately solves the two subproblems introduced previously, namely, the private power control P1.1 and the common rate allocation P1.2. To promote convergence and enhance numerical stability, the solution obtained from one subproblem in each iteration is used as the initial value for the subsequent subproblem. This warm-start strategy effectively reduces the number of iterations required and helps avoid suboptimal local points. After the alternating optimization process between \mathbf{r} and \mathbf{P}_r converges for a given P_0 , a one-dimensional search is performed over P_0 within its feasible domain to determine the value that minimizes the overall system latency. The corresponding optimal resource allocation, comprising both the power and rate vectors, is denoted as $(\mathbf{P}^*, \mathbf{r}^*)$. This hierarchical optimization structure, inner alternating optimization nested within an outer one, dimensional search ensures efficient and effective resource coordination under the coupled nature of the system constraints.

B. Pinching-Antenna Location Optimization

Under a fixed power allocation policy, the optimization problem for determining the optimal pinching-antenna position and common rate allocation can be formulated as follows. It is important to note that the antenna position x^{Pin} directly influences the channel gain of the user with the worst channel condition, thereby affecting the achievable common rate R_0 . This dependency creates a coupling between the antenna position and the common

rate allocation vector \mathbf{r} , necessitating their joint optimization. The resulting optimization problem is formally stated as:

$$\begin{aligned} \text{P2: } & \min_{x^{\text{Pin}}, \mathbf{r}} \max_{i \in \mathcal{I}(\mathbf{m})} \frac{c_i}{r_i + R_{i,r}(x^{\text{Pin}})} \\ \text{C2: } & \sum_{i \in \mathcal{I}(\mathbf{m})} r_i \leq B \log_2 \left(1 + \frac{P_0}{\sum_i P_i + \frac{\sigma^2}{h_0(x^{\text{Pin}})}} \right), \\ \text{C4: } & x^{\text{Pin}} \in [0, L], \\ \text{C6: } & r_i \geq 0, \quad i \in \mathcal{I}(\mathbf{m}). \end{aligned}$$

The direct solution of P2 presents significant challenges due to the strongly non-convex nature of the objective function and the intricate coupling between the optimization variables x^{Pin} and \mathbf{r} . The objective function incorporates a max-min fractional structure, while the constraint **C2** introduces a logarithmic relationship that depends nonlinearly on x^{Pin} through the worst-case channel gain $h_0(x^{\text{Pin}})$.

However, a key observation enables an efficient solution approach: for any fixed antenna position x^{Pin} , the problem reduces to a rate allocation subproblem that shares the same structural properties as the previously solved P1.2. This suggests a decomposition strategy where we: Leverage the one-dimensional nature of $x^{\text{Pin}} \in [0, L]$ by employing the golden-section search method, which is particularly effective for optimizing unimodal functions in one-dimensional spaces, even when the objective function lacks closed-form differentiability. For each candidate antenna position x^{Pin} evaluated during the golden-section search, solve the associated rate allocation subproblem:

$$\begin{aligned} \text{P2.1: } & \min_{\mathbf{r}} \max_{i \in \mathcal{I}(\mathbf{m})} \frac{c_i}{r_i + R_{i,r}(x^{\text{Pin}})} \\ \text{C2: } & \sum_{i \in \mathcal{I}(\mathbf{m})} r_i \leq B \log_2 \left(1 + \frac{P_0}{\sum_i P_i + \frac{\sigma^2}{h_0(x^{\text{Pin}})}} \right), \\ \text{C6: } & r_i \geq 0, \quad i \in \mathcal{I}(\mathbf{m}). \end{aligned}$$

P2.1 maintains a convex structure similar to P1.2, as analyzed previously, and can therefore be efficiently solved to global optimality using established convex optimization techniques, such as those implemented in the CVX framework.

The complete algorithm proceeds as follows: the golden-section search iteratively narrows down the interval for x^{Pin} based on objective function evaluations. At each evaluation point, the corresponding convex rate allocation subproblem P2.1 is solved to determine the achievable latency. This process continues until the search interval converges, ultimately identifying the optimal antenna position $x^{\text{Pin}*}$ and the corresponding rate allocation vector \mathbf{r}^* that collectively minimize the system latency. This decomposition approach effectively handles the non-convexity of the original problem while ensuring computational efficiency.

C. Joint Optimization Algorithm for P0

This subsection presents an alternating optimization algorithm designed to solve the original average latency minimization problem by jointly updating the variables x^{Pin} , \mathbf{r} , and \mathbf{P} . Let $x^{\text{Pin}}(t)$, $\mathbf{r}(t)$, and $\mathbf{P}(t)$ denote the antenna position, rate allocation, and power allocation in the t -th iteration, respectively. In addition, denote by $L(t)$ the average latency in the t -th iteration. For the specific request state \mathbf{m} , the proposed algorithm proceeds as follows: given the antenna location from the previous iteration, $x^{\text{Pin}}(t-1)$, we first compute $\mathbf{P}(t)$ and $\mathbf{r}(t)$ by solving P1, and obtain $L(t)$. Then, using the updated power allocation $\mathbf{P}(t)$, we jointly optimize the antenna position and rate allocation, yielding $x^{\text{Pin}}(t)$ and $\mathbf{r}(t)$ via P2, and obtain $L'(t)$. This iterative process continues until the improvement in average latency falls below a predefined threshold ϵ . By applying the described alternating optimization procedure to each possible request state $\mathbf{m} \in \mathbf{M}$, we can obtain the corresponding optimal solution tuple $(x^{\text{Pin}}(\mathbf{m}), \mathbf{P}(\mathbf{m}), \mathbf{r}(\mathbf{m}))$. Finally, the average system latency $L(x^{\text{Pin}}, \mathbf{P}, \mathbf{r})$ is computed by substituting these state-dependent solutions into the expectation formula given in (12). For clarity, the detailed procedure is summarized in Algorithm 2.

Algorithm 2 Joint Optimization Algorithm for P0

Require: Initial antenna location $x^{\text{Pin}}(0)$ and optimal solution tuples for all states $\mathbf{m} \in \mathbf{M}$:

- 1: for each request state $\mathbf{m} \in \mathbf{M}$ do
- 2: Set $t = 1$
- 3: Set $x^{\text{Pin}}(0) \leftarrow x^{\text{Pin}}(0)$ for current state \mathbf{m}
- 4: repeat
- 5: Update $\mathbf{P}(t)$ and $\mathbf{r}(t)$ by solving P1 under fixed $x^{\text{Pin}}(t-1)$
- 6: Compute average latency $L(t)$ using (11)
- 7: Update $x^{\text{Pin}}(t)$ and $\mathbf{r}(t)$ by solving P2 under fixed $\mathbf{P}(t)$
- 8: Compute updated average latency $L'(t)$ using (11)
- 9: $t \leftarrow t + 1$
- 10: until $|L(t) - L'(t)| \leq \epsilon$
- 11: Store optimal solution for state \mathbf{m} :
- 12: $x^{\text{Pin}}(\mathbf{m}) \leftarrow x^{\text{Pin}}(t)$, $\mathbf{P}(\mathbf{m}) \leftarrow \mathbf{P}(t)$, $\mathbf{r}(\mathbf{m}) \leftarrow \mathbf{r}(t)$
- 13: end for
- 14: Compute the average system latency $L(x^{\text{Pin}}, \mathbf{P}, \mathbf{r})$ by substituting these state-dependent solutions into the expectation formula given in (12)
- 15: return Optimal solution tuples
 $\{(x^{\text{Pin}}(\mathbf{m}), \mathbf{P}(\mathbf{m}), \mathbf{r}(\mathbf{m}))\}_{\mathbf{m} \in \mathbf{M}}$ and average latency $L(x^{\text{Pin}}, \mathbf{P}, \mathbf{r})$

The proposed alternating optimization algorithm iteratively updates the antenna location, power allocation, and rate allocation variables, ensuring that the average system latency is monotonically non-increasing in each iteration. Since the objective function is bounded below and the constraint set is closed and convex, the algorithm is guaranteed to converge to a stationary point.

V. Simulation Results

In this section, we conduct comprehensive numerical simulations to assess the performance of the proposed

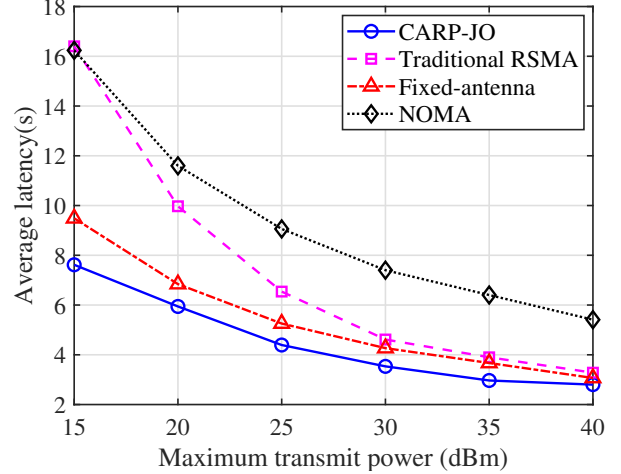


Fig. 2: System's average latency vs. the maximum transmit power of BS.

CARP-JO algorithm against several baseline schemes. The simulation parameters are configured as follows [13]: the carrier frequency is set to $f_c = 28$ GHz, the antenna height is $d = 3$ m, and the noise power is $\sigma^2 = -90$ dBm. Four users are randomly distributed within a rectangular service area of dimensions $D_x = 120$ m and $D_y = 40$ m. These users request content from a catalog comprising 30 items, with content sizes uniformly distributed between 1 and 20 Mbits. The system bandwidth is assumed as 1 MHz. The popularity of the files follows a Zipf distribution with an exponent of 0.5. The BS transmit power budget is constrained to $P_b = 25$ dBm, and the length of the dielectric waveguide is set to D_x . The simulation parameters are given in Table II.

TABLE II: Simulation Parameters

Parameters	Values
The carrier frequency f_c	28 GHz
The antenna height d	3 m
The noise power σ^2	-90 dbm
The length D_x and width D_y of the distribution range of users	120 m, 40 m
The number of contents	30
The exponent of the Zipf distribution	0.5
The transmit power budget of BS P_b	25 dbm

Performance comparisons are conducted against the following baseline methods:

- Traditional RSMA: This baseline employs the standard RSMA protocol [27] for content delivery without the proposed enhancements.
- NOMA: This approach substitutes RSMA with NOMA [28], while retaining the same caching strategy introduced in this work.
- Fixed-antenna: In this scheme, the antenna is statically positioned at $(0, 0, d)$ meters [13], and the system employs the proposed advanced RSMA mechanism.

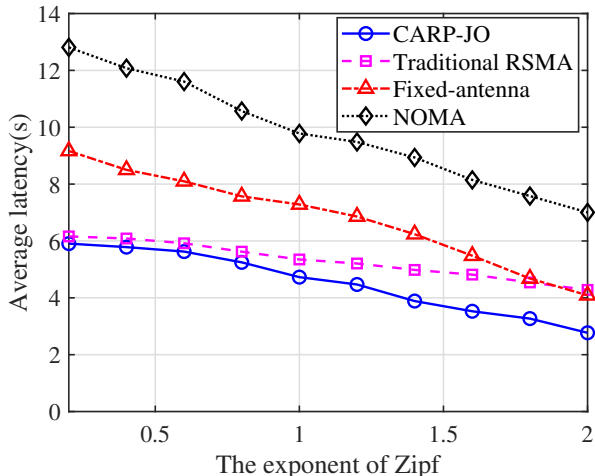


Fig. 3: System's average latency vs. the exponent of Zipf.

Fig. 2 demonstrates the superior performance of the proposed CARP-JO scheme, as it consistently achieves the lowest average latency across the entire range of BS transmit power when compared to the three baseline methods. For instance, when the total power is 15 dbm, our CARP-JO scheme saves the latency by 20%, 53%, 54% when compared to that of Fixed-Antenna, Traditional RSMA and NOMA, respectively. This performance gain is attributed to the joint optimization of the antenna's physical location and the enhanced RSMA resource allocation, which dynamically minimizes path loss by establishing superior LoS links and efficiently manages interference and power through content-aware private stream sharing. All schemes benefit from increased transmit power, exhibiting lower latency due to improved SNR and higher data rates. However, the proposed CARP-JO algorithm uniquely leverages the pinching antenna's flexibility to concentrate power and reduce spatial correlation. This enables it to significantly outperform conventional setups, particularly at low-to-moderate power levels.

Fig. 3 illustrates the average latency performance with different exponents of Zipf. The proposed CARP-JO scheme consistently achieves the lowest latency across the evaluated parameter range. Its advantages stem from the joint optimization of antenna positioning and its content-aware design, which is particularly effective when user requests are concentrated. A higher Zipf exponent leads to a more concentrated request pattern, increasing content redundancy; this scheme leverages that by having users requesting the same file share a private stream, drastically reducing interference and improving power efficiency. In contrast, the traditional RSMA scheme performs somewhat worse because it fails to exploit this content redundancy, inefficiently dedicating separate private streams to all users regardless of their requests, an approach whose inefficiency is exacerbated by a concentrated request pattern. The fixed-antenna scheme and the NOMA scheme perform even worse, which highlights the

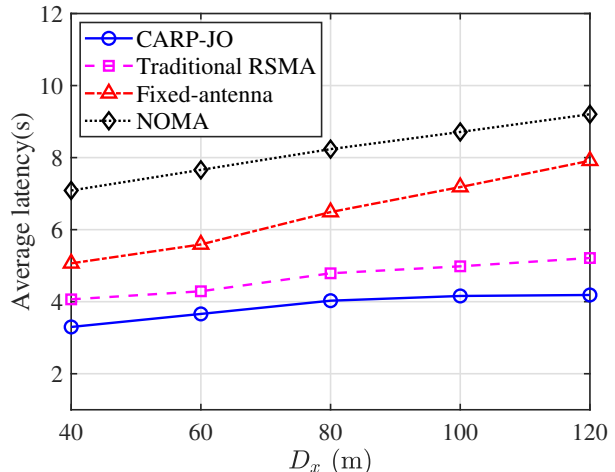


Fig. 4: System's average latency vs. D_x .

significant individual contributions of both the dynamic antenna positioning and the enhanced RSMA structure to the overall latency reduction.

Fig. 4 illustrates the system's average latency as a function of the service area length, D_x . The proposed CARP-JO scheme consistently achieves the lowest latency across the entire range of D_x values, demonstrating its robustness to changes in network coverage size. As D_x increases, the user distribution becomes more dispersed, leading to greater variation in path loss and a higher likelihood of poor channel conditions for edge users. The proposed CARP-JO scheme effectively mitigates this degradation through its dynamic antenna positioning, which optimizes the LoS link to the worst-case user, thereby improving the common stream rate R_0 . Concurrently, its content-aware design, which groups users requesting the same file onto a shared private stream, reduces inter-user interference and concentrates power, enhancing private rates $R_{i,r}$. In contrast, the performance of the fixed-antenna scheme degrades more noticeably as D_x grows, highlighting the critical role of antenna mobility in large cells. Although Traditional RSMA and NOMA also use a movable antenna, their performance is still hampered by their core protocols. Traditional RSMA inefficiently allocates separate streams without exploiting content redundancy, while NOMA's rigid SIC structure struggles with the significant channel disparity in larger networks. Consequently, even with antenna mobility, they cannot match the holistic interference management and efficiency of the proposed co-designed scheme.

Fig. 5 illustrates the system's average latency with different numbers of users. It demonstrates that the proposed CARP-JO scheme maintains the lowest average latency as the number of users increases. When there are only two users, the performance of several algorithms is comparable, as the probability of users requesting the same file is lower when the number of users is small. Moreover, the fixed-antenna scheme exhibits higher

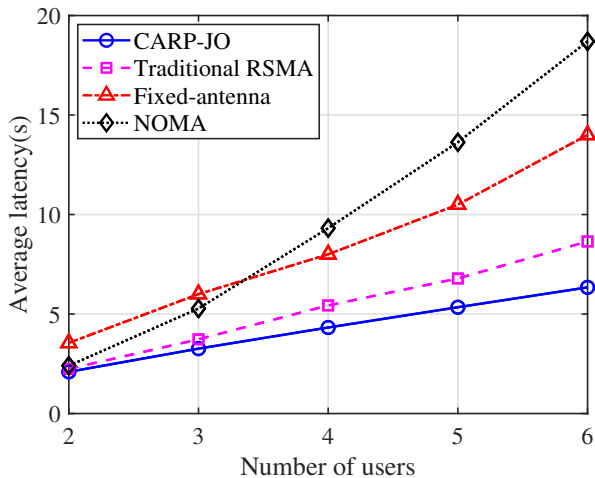


Fig. 5: System's average latency vs. the number of users

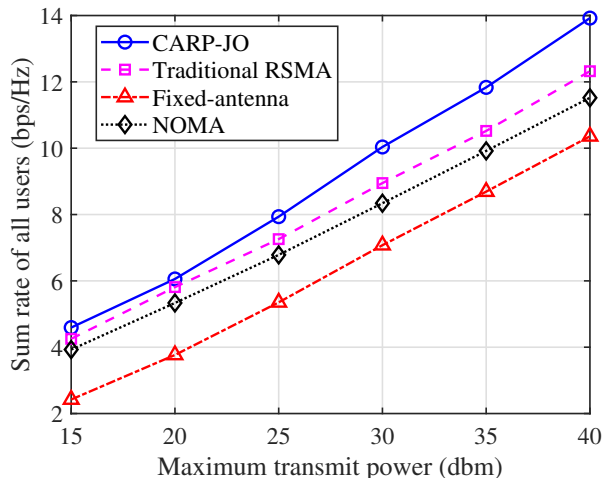


Fig. 7: Sum rate of all users vs. the maximum transmit power of BS.

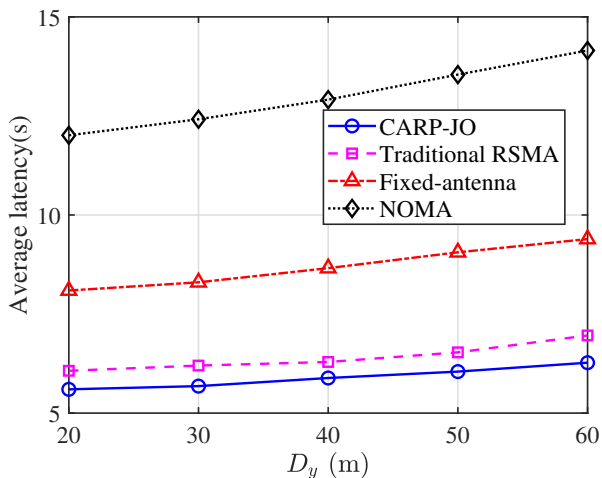


Fig. 6: System's average latency vs. D_y .

latency compared to the pinching-antenna approach. As the number of users increases, the advantage of our proposed CARP-JO algorithm becomes evident. This is because, as the number of users increases, the likelihood of users requesting the same files rises, resulting in greater redundant interference among them, and our proposed CARP-JO algorithm can effectively address this issue. In contrast, the performance of Traditional RSMA and NOMA degrades more noticeably due to their inefficient handling of interference and lack of holistic optimization, while the fixed-antenna scheme is fundamentally limited by its inability to adapt to the changing user topology.

Fig. 6 illustrates the average latency performance with different width of user distribution area (D_y). It shows that as D_y increases from 40m to 120m, the average latency rises for all four schemes, with the proposed CARP-JO scheme consistently maintaining the lowest latency. While all methods experience performance degradation with greater distance, the proposed CARP-JO scheme demonstrates superior robustness, as its latency increases

at a slower rate compared to Traditional RSMA, fixed-antenna configuration, and the significantly higher-latency NOMA baseline. When $D_y = 60\text{m}$, the CARP-JO scheme saves the latency by 10%, 33%, 56% when compared to that of Traditional RSMA, Fixed-Antenna and NOMA, respectively. This indicates that the proposed CARP-JO scheme is more effective in mitigating the adverse effects of increasing user distance, making it the most suitable for wide-area deployments.

Fig. 7 compares the sum rate of all users against the maximum transmit power for the proposed CARP-JO scheme and baseline methods. Notably, while NOMA exhibited the worst latency performance in our primary optimization, it surpasses the fixed-antenna baseline in terms of sum rate across most power levels. This occurs because the fixed-antenna system employs the proposed CARP-JO content-aware RSMA strategy, which is explicitly optimized for minimizing the maximum latency among all users. To achieve this, it prioritizes the user with the worst channel condition by allocating more resources, consequently limiting the rates achievable by users with better channels and thus reducing the overall sum rate. In contrast, the NOMA scheme, while not content-aware, benefits from the dynamic positioning of the pinching antenna, which improves channel conditions for all users. This allows NOMA to more effectively leverage its power-domain multiplexing to boost aggregate throughput, albeit at the cost of high latency and unfairness, as shown in our primary results. Strikingly, the Proposed CARP-JO scheme transcends this trade-off. By synergistically co-designing the dynamic pinching antenna with the content-aware RSMA, it simultaneously achieves the highest sum rate and the lowest latency, demonstrating that intelligent physical layer and link layer integration can optimize both metrics concurrently.

VI. Conclusion

This paper presented a novel content-aware RSMA-enabled pinching-antenna framework for downlink multicast systems, which integrates dynamic antenna positioning with content-sensitive transmission to minimize average latency. Within this architecture, we formulated a joint optimization problem that co-designs the physical placement of the pinching antenna and the RSMA resource allocation parameters to minimize system latency. Due to the non-convex and coupled structure of the problem, CARP-JO algorithm was developed, decomposing the original problem into tractable subproblems. RSMA resource allocation is addressed via a combination of bisection search and convex optimization, while antenna positioning is efficiently optimized using the golden-section search method. Extensive simulations validate that the proposed CARP-JO scheme consistently outperforms conventional RSMA, NOMA, and fixed-antenna systems under diverse scenarios, including variations in transmit power, user density, coverage size, and content popularity distribution. Future work will focus on extending multi-waveguide configurations, developing low-complexity algorithms for real-time applications, and ensuring robust operation under imperfect channel state information.

References

- [1] H. O. Y. Suzuki and K. Kawai, "Pinching antenna: Using a dielectric waveguide as an antenna," *NTT DOCOMO Technical J*, vol. 23, no. 3, pp. 5–12, Jan. 2022.
- [2] Z. Yang, N. Wang, Y. Sun, Z. Ding, R. Schober, G. K. Karagiannidis, V. W. Wong, and O. A. Dobre, "Pinching antennas: Principles, applications and challenges," *arXiv preprint arXiv:2501.10753*, 2025.
- [3] Y. Wang, Y. Liu, Y. Fu, and Z. Ding, "Pinching-antenna systems for indoor immersive communications: A 3d-modeling based performance analysis," *IEEE Wireless Communications Letters*, Mar. 2025.
- [4] B. Rimoldi and R. Urbanke, "A rate-splitting approach to the Gaussian multiple-access channel," *IEEE Transactions on Information Theory*, vol. 42, no. 2, pp. 364–375, Mar 1996.
- [5] Y. Mao, B. Clerckx, and V. O. Li, "Rate-splitting multiple access for downlink communication systems: bridging, generalizing, and outperforming SDMA and NOMA," *EURASIP journal on wireless communications and networking*, vol. May 2018, no. 1, pp. 1–54, 2018.
- [6] Z. Ding, R. Schober, and H. Vincent Poor, "Flexible-antenna systems: A pinching-antenna perspective," *IEEE Transactions on Communications*, pp. 1–1, 2025.
- [7] Y. Xu, Z. Ding, and G. K. Karagiannidis, "Rate maximization for downlink pinching-antenna systems," *IEEE Wireless Communications Letters*, vol. 14, no. 5, pp. 1431–1435, May 2025.
- [8] K. Wang, C. Ouyang, Y. Liu, and Z. Ding, "Pinching-antenna systems with los blockages," *IEEE Wireless Communications Letters*, pp. 1–1, Sept. 2025.
- [9] Z. Ding and H. Vincent Poor, "Los blockage in pinching-antenna systems: Curse or blessing?" *IEEE Wireless Communications Letters*, vol. 14, no. 9, pp. 2798–2802, Sept. 2025.
- [10] J. Zhang, H. Xu, C. Ouyang, Q. Zou, and H. Yang, "Uplink sum-rate maximization for pinching antenna-assisted multiuser miso communications," *IEEE Communications Letters*, pp. 1–1, Sept. 2025.
- [11] Z. Wang, C. Ouyang, Y. Liu, and A. Nallanathan, "Wireless sensing via pinching-antenna systems," *IEEE Wireless Communications Letters*, pp. 1–1, Aug. 2025.
- [12] Y. Qin, Y. Fu, and H. Zhang, "Joint antenna position and transmit power optimization for pinching antenna-assisted isac systems," *IEEE Wireless Communications Letters*, pp. 1–1, Aug. 2025.
- [13] M. Zeng, J. Wang, X. Li, G. Wang, O. A. Dobre, and Z. Ding, "Sum rate maximization for noma-assisted uplink pinching-antenna systems," *arXiv preprint arXiv:2505.00549*, 2025.
- [14] K. Wang, Z. Ding, and R. Schober, "Antenna activation for noma assisted pinching-antenna systems," *IEEE Wireless Communications Letters*, vol. 14, no. 5, pp. 1526–1530, May 2025.
- [15] Y. Fu, F. He, Z. Shi, and H. Zhang, "Power minimization for noma-assisted pinching antenna systems with multiple waveguides," in *GLOBECOM 2025 IEEE Global Communications Conference*, 2025.
- [16] Y. Li, H. Xu, M. Zeng, and Y. Liu, "Pinching antenna-aided wireless powered communication networks," *IEEE Wireless Communications Letters*, pp. 1–1, Oct. 2025.
- [17] Y. Saito, Y. Kishiyama, A. Benjebbour, T. Nakamura, A. Li, and K. Higuchi, "Non-orthogonal multiple access (noma) for cellular future radio access," in *2013 IEEE 77th Vehicular Technology Conference (VTC Spring)*, june 2013, pp. 1–5.
- [18] X. Lyu, S. Aditya, J. Kim, and B. Clerckx, "Rate-splitting multiple access: The first prototype and experimental validation of its superiority over sdma and noma," *IEEE Transactions on Wireless Communications*, vol. 23, no. 8, pp. 9986–10000, Aug. 2024.
- [19] U. Ali, L. De Nardis, and M.-G. Di Benedetto, "Energy efficiency and fairness in large scale systems using rsma," *IEEE Open Journal of the Communications Society*, vol. 6, pp. 611–628, Jan. 2025.
- [20] X. Lyu, S. Aditya, and B. Clerckx, "Rate-splitting multiple access for overloaded multi-group multicast: A first experimental study," *IEEE Transactions on Broadcasting*, vol. 71, no. 1, pp. 30–41, Mar. 2025.
- [21] X. Liu, J. Feng, F. Li, and V. C. M. Leung, "Downlink energy efficiency maximization for rsma-uav assisted communications," *IEEE Wireless Communications Letters*, vol. 13, no. 1, pp. 98–102, Jan. 2024.
- [22] J. Hu, G. Liu, Z. Ma, M. Xiao, and P. Fan, "Low-complexity resource allocation for uplink rsma in future 6g wireless networks," *IEEE Wireless Communications Letters*, vol. 13, no. 2, pp. 565–569, 2024.
- [23] X. Dong, C. Zhan, X. Meng, and Y. Mu, "Dynamic resource management for rsma-enabled uav networks with mobile users," *IEEE Transactions on Vehicular Technology*, vol. 74, no. 10, pp. 16447–16452, Oct. 2025.
- [24] P. Wang, H. Wang, and R. Song, "Sum rate maximization for pinching antennas assisted rsma system with multiple waveguides," 2025. [Online]. Available: <https://arxiv.org/abs/2506.10596>
- [25] A. A. Tegós, Y. Xiao, S. A. Tegós, G. K. Karagiannidis, and P. D. Diamantoulakis, "Uplink rsma for pinching-antenna systems," 2025. [Online]. Available: <https://arxiv.org/abs/2509.10076>
- [26] L. Breslau, P. Cao, L. Fan, G. Phillips, and S. Shenker, "Web caching and Zipf-like distributions: evidence and implications," in *IEEE INFOCOM*, vol. 1, Mar. 1999, pp. 126–134.
- [27] Z. Yang, M. Chen, W. Saad, and M. Shikh-Bahaei, "Optimization of rate allocation and power control for rate splitting multiple access (RSMA)," *IEEE Transactions on Communications*, vol. 69, no. 9, pp. 5988–6002, Sep. 2021.
- [28] Z. Shi, H. Wang, Y. Fu, G. Yang, S. Ma, F. Hou, and T. A. Tsiftsis, "Zero-forcing-based downlink virtual MIMO-NOMA communications in IoT networks," *IEEE Internet of Things Journal*, vol. 7, no. 4, pp. 2716–2737, Apr. 2020.